HIGH REPETITION HIGH PERFORMANCE PLASMA FOCUS AS A POWERFUL RADIATION SOURCE

S. Lee, P. Lee[1], G. X. Zhang, V. A.Gribkov[2], X. Feng, M. H. Liu and A.Serban[1]
School of Science, Nanyang Technological University
National Institute of Education
469 Bukit Timah Rd, Singapore 259756

[1] School of Electrical & Electronic Engineering, Nanyang Technological University
[2] P.N. Lebedev Physical Institute, Russian Academy of Sciences, Moscow
leesing@optusnet.com.au

ABSTRACT

Basic operational characteristics of the plasma focus are considered from design perspectives to develop powerful radiation sources. Using these ideas we have developed two Compact Plasma Focus (CPF) devices operating in neon with high performance and high repetition rate capacity for use as an intense Soft X-ray (SXR) source for microelectonics lithography. The NX1 is a four-module system with a peak current of 320 kA when the capacitor bank (7.8μFx4) is charged to 14kV. It produces 100J of SXR per shot (4% wall-plug efficiency) giving at 3 Hz, 300W of average SXR power into 4π. The NX2 is also a four-module system. Each module uses a rail-gap switching 12 capacitors each with a capacity of 0.6μF. The NX2 operates with peak currents of 400kA at 11.5kV into water-cooled electrodes at repetition rates up to 16 Hz to produce 300W SXR in burst durations of several minutes. SXR lithographs are taken from both machines to demonstrate that sufficient SXR flux is generated for an exposure with only 300 shots. In addition flash electron lithographs are also obtained requiring only 10 shots per exposure. Such high performance compact machines may be improved to yield over 1 kW of SXR, enabling sufficient exposure throughput to be of interest to wafer industry. In deuterium the neutron yield could be over 10^{10} neutrons per sec over prolonged bursts of minutes.

INTRODUCTION

For Mather's type plasma focus operation it is observed experimentally /1,2/ that the quantity designated as the drive parameter /2/ $S=(I/a)/\rho^{½}$ (where I is the driving current and r the operational gas density), a measure of speed, both axial and radial, has an optimum value for each gas of operation. Thus for deuterium the average axial speed for optimum neutron yield appears to be just below 6 cm/μsec corresponding to a peak axial speed of 9-10 cm/μsec and a peak radial speed of some 25 cm/μsec as the plasma focus radial shock goes on axis. That the optimum speed should be so low for optimum neutron yield is surprising since one would expect from D-D fusion cross-section consideration that the fusion yield should be enhanced by an increase in speed which should boost the focus ions above the 1 keV observed for focus operation at the above mentioned optimum speeds. The speed limitation may be caused by a force-field flow-field decoupling effect /1/. An effort to achieve yield enhancement by breaking through the speed limit has been made /3/.

Operating in noble gases for the generation of soft x-ray (SXR) an optimum speed may be more readily understood. For example in neon the compressed plasma in the focus should have a temperature of some 400 eV if the radiation is required to be predominantly in the 0.8-1.4 nm for the purpose of microelectronics lithography. We have used a model computing plasma dynamics in the axial, radial, and radial reflected shock phases, incorporating a quasi-equilibrium radiative phase /4,5,6/ to examine for example the optimum axial speed required to set the stage for optimum radiation in the 0.8-1.4 nm range. This model is used to correlate with experimental results which indicate an optimum average axial speed of 4.5 cm/μsec.

It is important to note that the optimum speed for each of deuterium and neon operation remains nearly contant for the range of machines surveyed. This is particularly remarkable for deuterium operation where a value of S nearly constant at 90 kA/torr^{½} , corresponding to a peak axial speed of just less than 10 cm/μsec, is tabulated /1/ over a wide range of machines from training machines of 3 kJ /2/ to machines of 300kJ. This means that for each gas the plasma temperatures in each of the dynamic phases, and by inference also in the compressed radiative phase, are identical for all machines, big and small, when optimized.

We next note that the quantity S is dependent on D=(I/a) linearly whilst it depends only on the half power of ρ. Note also that over a two decade range of stored energy the optimized operational pressure has a range of only 2 /1/. Thus in a relative sense the density ρ and hence the quantity D may in the first approximation be considered also as constant when comparing different machines, all optimized. This clearly agrees with the design tendency to increase the anode radius proportionally with the available drive current. But there is also a fundamental significance.

For each gas, since we are dealing with the same compressed temperature and essentially the same density, radiation yield will depend on the product of compressed plasma volume and lifetime. Again since we are dealing with the same dynamical speeds and compressed temperatures any reasonable modelling /4,7,14/ will show that each dimension of the pinched plasma is proportional to the anode radius, as is the lifetime of the compressed plasma. Thus radiation yield is proportional to a^4. And since D is essentially constant for each gas, radiation yield, at least for neutrons and SXR, is proportional to I^4. Such a scaling is energetically possible since whenever energy is taken from the circuit by the plasma such an energy extraction will reflect in a lowering of the current. Such a self-regulating mechanism will self-consistently limit the extraction of energy from the circuit.

Thus for a given stored energy, yield performance is related to current. Circuit inductance needs to be minimized. Our modelling also indicates the importance of minimizing the ratio of generator impedance to total impedance for efficient transfer of energy to the plasma pinch. Practically this is again accomplished by minimizing all the inductances from the capacitor bank through the switches right up to the collector flanges of the plasma focus head. Thus improving circuit performance should improve yield performance.

For applications, whilst the peak rates of yield may have significance for some time-resolved experiments, for other applications such as SXR lithography for microelectronics application there is a need for high average yield rates sustained over at least a duration of minutes, even for demonstration purposes. Thus ability to operate at high repetition rates in a prolonged burst is necessary.

The length of the anode is also of crucial importance /2,7/. Computation and experience agree that a strong focus with optimum energy coupled into the focus pinch so as to emit intense radiation, is achieved when the radial compression starts (end of axial phase) at a time t_{ax} where t_{ax} is equal to t_r, t_r being a hypothetical risetime of the capacitor bank with a value between the short-cicuited risetime and the risetime of the circuit loaded hypothetically with the full axial load. As a rule of thumb the short-circuited risetime may be used for a first estimate of the optimum anode length.

Thus for the deuterium focus with an optimum average axial speed of say 5.5 cm/μsec the anode length should be 5.5 cm per μsec short-circuited bank ristime. For the neon focus taking the optimum average axial speed to be 4.5 cm/μsec would give us an indicative optimum anode length of 4.5cm for every μsec of shortcuited bank risetime.

What about the value of D=(I/a)? From a survey of experiments it is found that the current per unit anode radius has a design range of 150-220 kA/cm, for optimum neutron yield. We have used this range also as an indicative design range for our SXR facilities.

Based on the above considerations we have developed two high repetition rate compact plasma focus facilities, the NX1 and the NX2 to be powerful SXR sources for microelectronics lithography /8,9,10/.

We note that the requirements for a point SXR lithography source may be expressed as follows: point source dimension less than 1 mm (focussed plasma viewed end-on) with emission in the wavelength range 0.8-1.4nm, and average SXR power of 1 kW at source over 4π delivered over a prolonged burst. This last requirement indicates what is needed from industrial wafer throughout considerations. For a resist with 100mJ/cm^2 sensitivity exposed at a distance which cannot be less than 30cm /9/ from the point source, 1kW will deliver the required 100 mJ/cm^2 in 2 sec assuming beamline transmission ratio of 0.5. A 2 sec exposure time per field may be sufficient for industrial wafer throughput purposes. For demonstration purposes even a 100W source is useful.

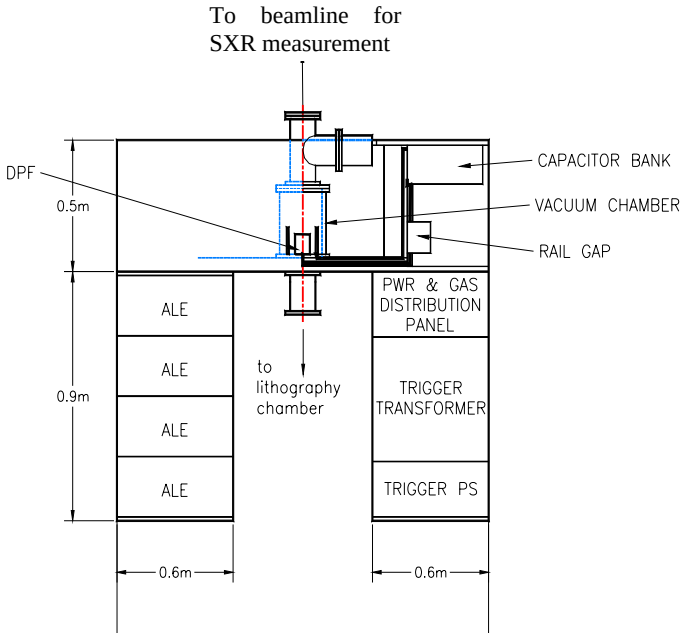

Figure 1 General overview of the NX2 apparatus

Other practical design features include compact footprint with ample space for a stepper to be integrated eventually into the facility.

2. APPARATUS

The plasma focus soft x-ray sources used in these experiments are low energy ~2kJ plasma focus operated in neon. A general view of the NX2 is shown in Fig 1. The design enables measurement of SXR yield at the same time as lithographic exposure is made. The footprint of the machine is 1.6 m x 1.6 m. There is a clear space for the integrated development of a stepper. The system is completely shielded against electromagnetic radiation.

2.1 Electrical system

Both the NX1 and NX2 plasma focuses are driven by 30μF capacitor bank charged by ALE Systems model 802 high voltage capacitor chargers. The capacitor banks are connected to the focus via four switches (pseudo spark switches for the NXI and rail gap switches for the NX2). Table 1 summarizes the characteristics of the electrical systems. A schematic of the electrical system is shown in Fig 2.

	Charging Voltage (kV)	Energy (kJ)	Repetition rate (Hz)	Current (kA)	Short circuit rise time or quarter period (μs)
NX1	12	2.2	3*	280	1.5
NX2	11.5	1.9	16	400	1.0

Table 1 Summary of electrical characteristics *** limited by available charging power.**

2.2 Focus chamber

Three chambers have been used in the NX1 (see Fig 3) with oxygen-free copper anode lengths 3.5, 4.5 and 5.5 cm respectively. Three anode lengths were tried with the NX2. The electrode dimensions are summarized in table 2. The NX2 stainless steel electrodes are cooled by water circulated through the electrodes using two Bay Voltex RRS-1650-AC chillers with a total cooling capacity of 9.6kW

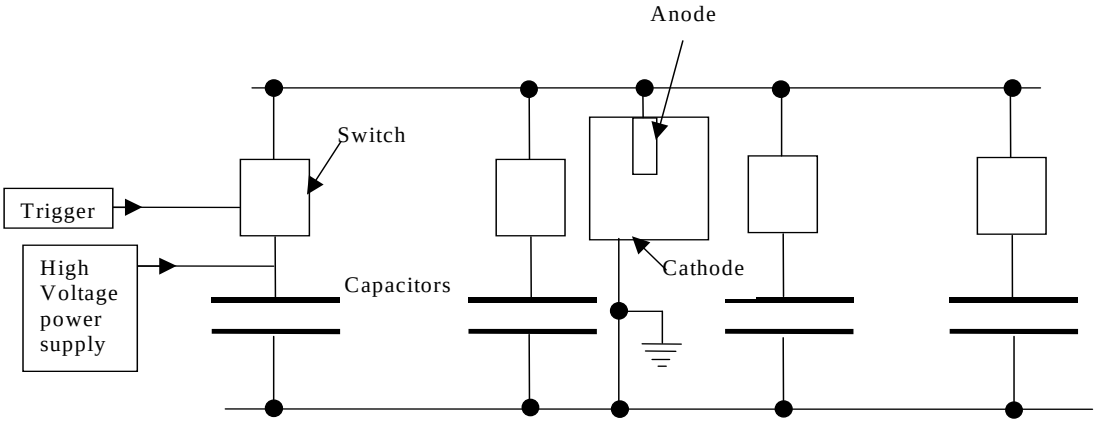

Figure 2. Schematic of electrical system

.

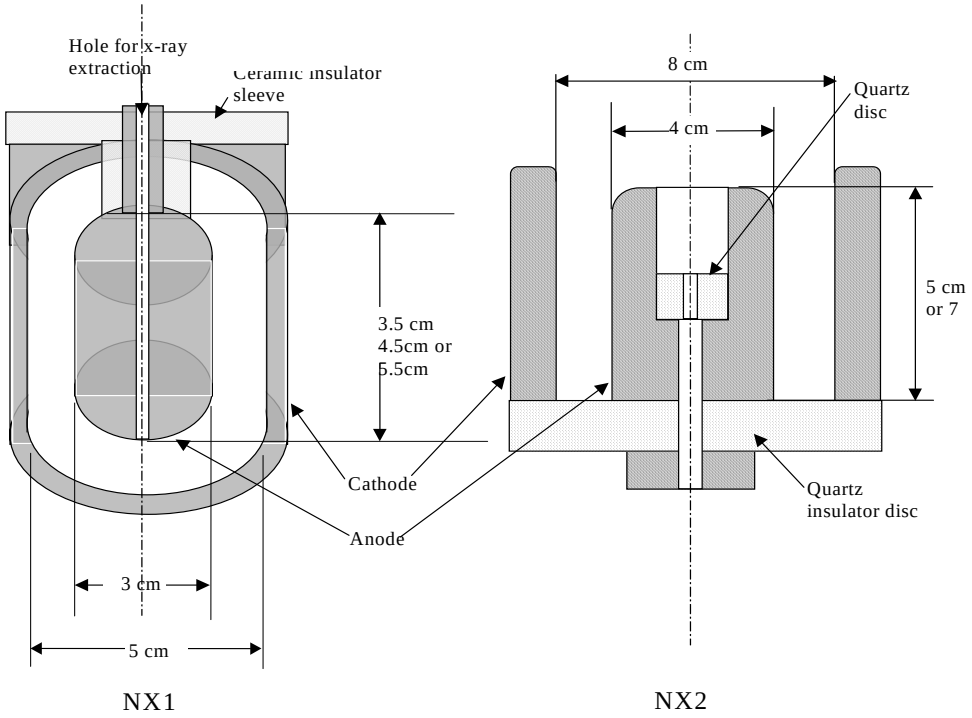

Figure 3. Schematic of focus electrodes and chamber

	Anode diameter(cm)	Cathode diameter (cm)	Anode length (cm)	Electrode material	Insulator material
NX1	3	5	3.5, 4.5, 5.5	Copper	Ceramic
NX2	4	8	5, 7	Stainless steel	Quartz

Table 2 Summary of focus electrodes

3. EXPERIMENT

The diagnostics were 1mm^2 area 10μm thick PIN diodes and 3mm^2 photoconducting diamond (PCD) filtered by aluminium, mylar and beryllium foils. The setup used for the experiments is shown in Fig 4. Both the PCDs and the PIN diodes were used on both machines. In the case of the NX1, the x-ray was

detected through the extraction hole through the anode. This means that there is also an electron beam travelling along the same path. The electrons are excluded by the application of a magnetic field to deflect the electrons and also by the 10 μm beryllium which scatters the electrons. The energy of the electrons have been determined in a previous experiment /11/.

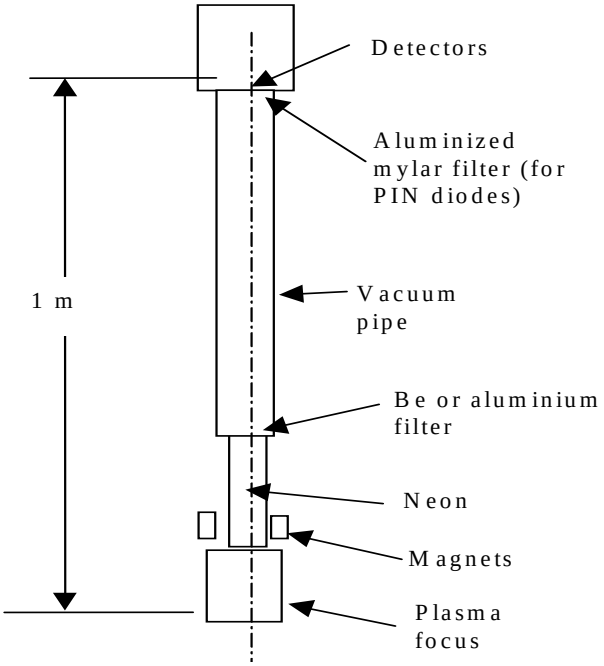

Figure 4 Experimental set up for soft x-ray measurement

The initial pressure of neon was varied and the optimum pressure was found for the various electrode lengths and for charging voltages of 10kV and 14kV. Most of the datapoints were repeated 5-10 times for the NX1 and 20-200 times for the NX2. A fast acquisition system consisting of a tektronix TDS380 oscilloscope connected to a computer was used so that the x-ray for every shot up to a repetition rate of about 10 HZ could be obtained.

4. RESULTS

To obtain the SXR yield from the PIN diode pulse, the area under the oscilloscope trace is obtained and the total amount of SXR is calculated using a sensitivity factor into which has been folded the sensitivity versus wavelength characteristics of the PIN diode, the spectrum of the neon focus emission which had been separately obtained earlier using a crystal spectrograph /6/ and the absorption of the beamline gas path and filters. The PIN diode measurements are cross-calibrated against a calibrated PCD detector. The PCD has a flat sensitivity over the range of SXR spectrum considered. Hence interpretation of the yield is more reliable. The measurements using the two detectors agree to within 20% on the NX2. All results are adjusted to the PCD calibration.

The results from the x-ray yield measurements are shown in Fig 5. Fig 5a shows that with the NX1, we obtained up to 5% conversion into soft x-ray from the capacitor bank energy and corresponding wall plug efficiency of 4% with the 4.5cm anode at 12kV. The x-ray yield varies within 50% of the maximum when the pressure is within 20% of the optimum. The typical variation of the x-ray yield when other factors like neon pressure, charging voltage are kept constant is about ±35% of the average x-ray yield.

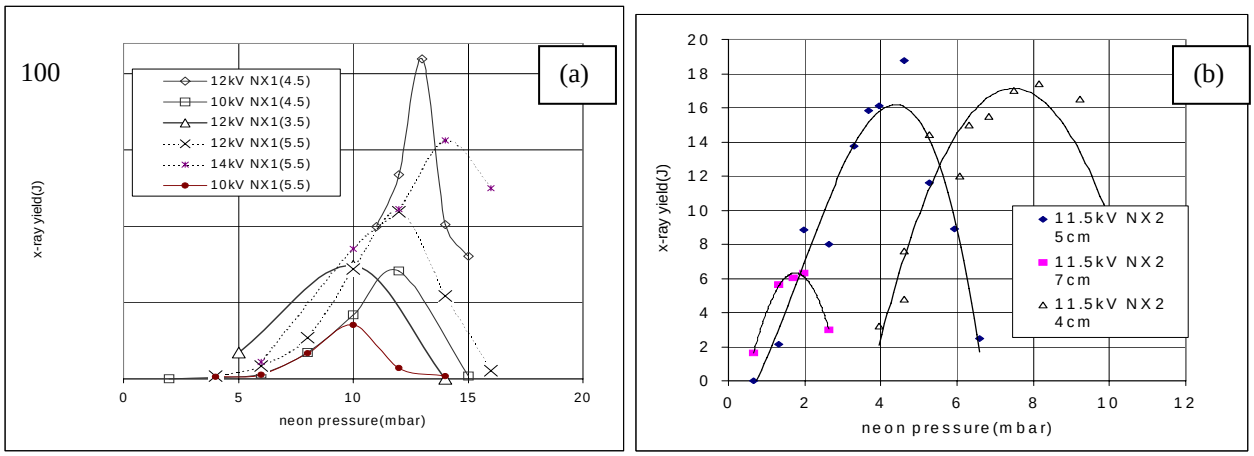

Figure 5. X-ray yield for different neon pressures for a) NX1 and b) NX2.

Figure 6 shows some representative oscilloscope current traces obtained using the NX1 with 4.5cm anode operated with a charging voltage of 10kV and the NX2 with the 5cm anode operated at 11.5kV with 4mbar neon. Some current dips to as low as 60% of the peak current when there are multiple focus within a short time of each other. More typical dips drop the current to 80% of the maximum which is what the 1st dip associated with the 1st focus event in figure 6a. It can be seen that the energy transfer into the plasma is more efficient for the NX2 as the dip shown in figure 6b dips to about 65% of the peak current with only one focus event.

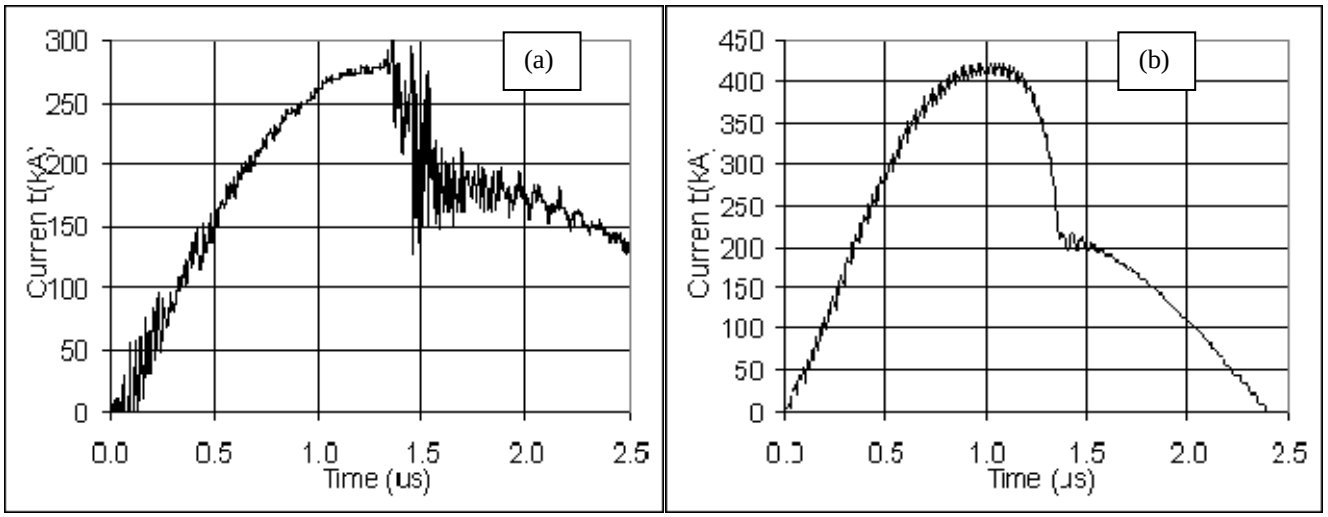

Figure 6 Some representative oscilloscope traces obtained from (a) the NX1 and (b) the NX2

Table 3 shows the parameters for maximum x-ray yield for some of the configurations we tried. It can be seen that the best SXR yield is at an average velocity of 4.5 μscm^{-1}. With the shorter electrode, it is not possible to run the focus at a higher velocity as the focus would occur at a time too long before the natural current peak such that not enough of the capacitor bank energy has been converted to the magnetic field energy driving the plasma. However if the anode is made too long and the velocity pushed too high, the final focus temperature will become too high for efficient production of neon K shell lines.

Mac-hine	Bank Voltage/ Energy (kV/kJ)	Length/ Equival-ent * (cm/cm)	Opti-mum Pressure (mbar)	Meas-ured Current (kA)	t_{ax} ** (μs)	Average Axial Speed ($cm\mu s^{-1}$)	D ($kAcm^{-1}$)	S (kA cm^{-1} $torr^{-1/2}$)	SXR yield (J)
NX1	10/1.5	5.5/6	10	230	1.50	4.0	153	56	20
NX1	12/2.2	5.5/6	12	280	1.45	4.1	187	62	55
NX1	14/2.9	5.5/6	14	320	1.40	4.3	213	66	80
NX1	10/1.5	4.5/5	12	230	1.25	4.0	153	56	35
NX1	12/2.2	4.5/5	13	280	1.10	4.6	186	60	105
NX1	12/2.2	3.5/4	10	280	1.10	3.6	187	68	35
NX2	11.5/1.9	7	2	340	1.30	5.4	170	139	7
NX2	11.5/1.9	5	4	400	1.15	4.4	200	115	18
NX2	11.5/1.9	4	7	410	1.05	3.8	205	90	15

Table 3 Comparative performance of NX1 and NX2

***The equivalent length takes into account that the NX1 is curved so that the run down length is slightly longer.**
****t_{ax}=time at end of axial phase, or start of compression, taken as 0.25/0.3 us before SXR pulse for the NX1/NX2.**

Figure 7 shows SXR lithographic exposures to confirm the SXR flux of NX1 and NX2 /12/. The resists used have a sensitivity rated at 100mJ/cm^2 and are placed 40cm from the focus. Magnets are placed to deflect the electron beams associated with the plasma focus /13/ to ensure that the exposure are by SXR. The mask is a 1 μm thick gold mesh with grid separation of 5 μm. The NX1 beamline has a 3 times poorer transmission ratio than the NX2 beamline. These lithographs confirm that the NX1 produces more than 3 times the SXR yield per shot when compared to the NX2.

Figure 8 shows a flash electron lithograph exposed on PMMA with 10 shots of NX1. For electron lithographs the deflecting magnets were removed. The exposure was used to estimate the electron beam current as 50μA over the 5 Hz burst . The electron energy was estimated as 30keV /12/.

5. CONCLUSION

We note that the NX1 and the NX2 have quite different yield performance. For each machine the observed speed at optimum yield for each anode length generally does correlate with the drive parameter S. However the value of S is significantly higher (up to 2 times) for equivalent speeds for the NX2 compared with the NX1. On the basis of machine scaling for neutrons /1/ we would have expected constant value of S for optimum operation. This difference may be the cause of the large difference in yield. Despite higher circuit performance the yield performance of the NX2 is significantly lower than the NX1. This may be due to the significantly lower value of S for the NX1 which could be related to a higher operational density (up to 3 times) of NX1 for equivalent speeds and D, when compared to the NX2. The higher optimum operational density at equivalent temperatures obviously favours a higher SXR yield for NX1. This yield superiority of NX1 could perhaps be ascribed to differences in electrode materials (oxygen-free copper for NX1 compared to stainless steel for the NX2), chamber configurations (carefully shaped channel and closed outer electrode for the NX1), perhaps even to the differences in backwall insulation materials and configuration.

In any case it appears that the NX1 chamber has the more promising features with maximum SXR yield over 100J and wall plug efficiency of 4%, compared to 18J and 1% for the NX2. By incorporating cooling in the NX1 chamber and increasing the charging capacity so that the NX1 chamber may be fired at 10Hz, 1kW of SXR power may be achieved which will expose a field at 30cm in less than 2sec on a 100mJ/cm^2 resist, assuming a beamline transmission of 0.5. This should be sufficient for industrial throughput demands applied to microelectronics lithography aimed at 0.15μm design rules.

Moreover, by using deuterium we expect a neutron yield of better than 10^9 per shot and 10^{10} neutrons per shot when operating the cooled NX1 in a prolonged burst at 10Hz. Such a powerful compact neutron source will have interesting applications.

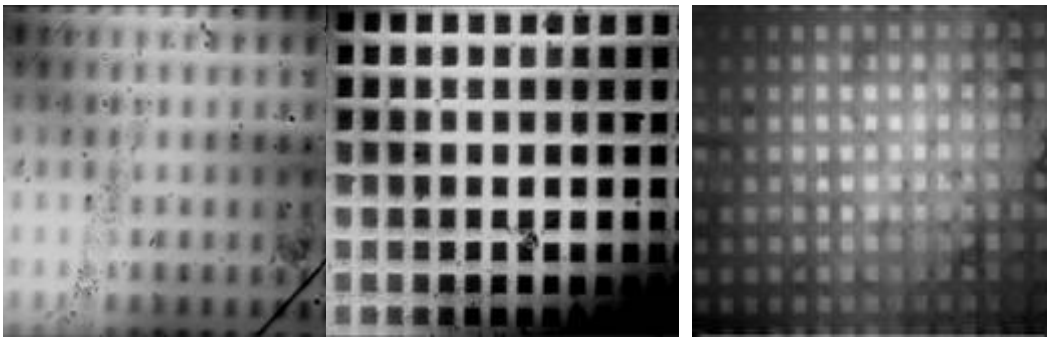

Figure 7 Test exposure (a) NX1 (200 shots & 400 shots) and (b) NX2 (300 shots)

Resist has a rated sensitivity of 100mJ/cm^2

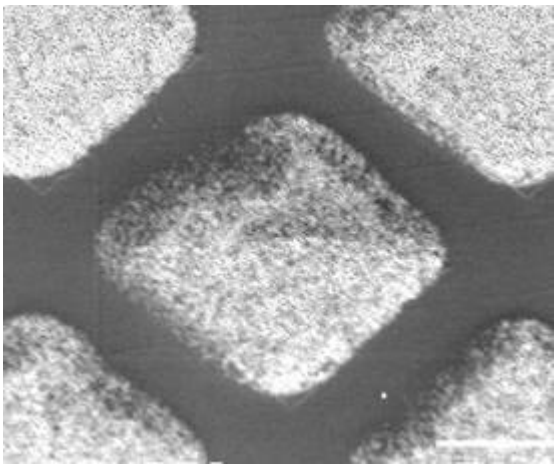

Figure 8 Flash electron lithograph on PMMA, 10 shots (NX1)

ACKNOWLEDGEMENTS

This work was supported by research grants of NTU and NIE ARC5/94 and RP9/94LS, and IAEA contract under CRP .

REFERENCES

1. S.Lee, A.Serban, Dimensions and lifetime of the plasma focus pinch, *IEEE Trans Plasma Sc*, **24**(3) 1101-1105 (1996)
2. S.Lee et. Al, A simple Facility for the teaching of plasma Dynamics and Plasma Nuclear Fusion. *American J. Phys*., **56**, 62-68 (1988)
3. S. Lee, A. Serban, Speed-enhanced Neutron Yield in Plasma Focus, *International Conf on Plasma Physics*, Foz do Iguassu, Brazil, Oct 1994 *Conf. Procs* **1**, 181-184 (1994)
4. S. Lee, A sequential Plasma Focus, *IEEE Trans Plasma Sc* **19**, 912-919 (1991)
5. S.Lee, Factors Limiting Compressions- Applications to the Radiative Plasma Focus, *International Conf on Plasma Sc & Tech*, Chengdu, P.R. China, June 1994 (ICPST '94) *Conference Digest* 71 (1994)
6. Liu Mahe, Soft x-rays from Plasma Focus, *PhD Thesis*, NTU, Singapore (1996)
7. S. Lee, Technology of a small Plasma Focus in *Small Plasma Experiments II*, Ed S. Lee & P.H. Sakanaka, World Scientific Co, 113-169 (1990)
8. E. Cullmann, T Kunneth, W. Neff, K.H. Stephan, Comparison of Different x-ray Sources using the Same Printing Process Parameters, *J. Vac Sci. Technol* **135**(3), 638-640 (1987)
9. Rahul R. Prasad, Mahadevan Krishnan et al, Neon Dense Plasma Focus Point X-ray source for < 0.25μm Lithography, *SPIE* **2194**, 120-128 (1994)
10. Y. Kato, S.H. Be, Generation of Soft X-ray using a Rare Gas-hydrogen Plasma Focus and its Applications to X-ray Lithography, *App. Phys. Lett*. **48**, 686-688 (1986)
11. P. Lee X. Feng, G.X. Zhang, S. Lee, Electron Lithography using a Compact Plasma Focus, accepted to be published by *Plasma Sources, Sci & Tech* (1997)
12. S. Lee, P. Lee et al, Preliminary Results on x-ray Lithography using a Compact Plasma Focus, accepted, *International Symp on Microelectronics Assembly ISMA '97*, Singapore, June 1997.
13. J.R. Smith, C.M. Luo, M.J. Rhee, R.F. Schneider, *Phys Fluids* **28**, 2305 (1985)
14. S. Lee, Energy Balance and the Radius of Electromagnetically Pinched Plasma Columns, *Plasma Phys* **25**, 571-576 (1983)